Journal of Power Sources 195 (2010) 5094–5100

Contents lists available at ScienceDirect

Journal of Power Sources

journal homepage: www.elsevier.com/locate/jpowsour

Synthesis and characterization of spherical nonstoichiometric $Ni(OH)_x$ ($x = 2.03–2.10$) as electrode materials

Guoxia Yuan, Kelong Huang*, Suqin Liu, Yajuan Li, Haiyan Wang

College of Chemistry and Chemical Engineering, Central South University, Changsha 410083, China

ARTICLE INFO

Article history:
Received 28 October 2009
Received in revised form 11 February 2010
Accepted 18 February 2010
Available online 24 February 2010

Keywords:
Nickel oxyhydroxide
Nickel hydroxide
Nickel–metal hydride batteries
High-rate discharge
Nonstoichiometric

ABSTRACT

The spherical nonstoichiometric $Ni(OH)_x$ ($x = 2.03–2.10$), as a new positive electrode material for Ni/MH batteries, are synthesized by spherical β-$Ni(OH)_2$ surface modified with chemically oxidized NiOOH nanoparticles. The average nickel oxidation state, microstructure and morphology of the spherical nonstoichiometric $Ni(OH)_x$ are investigated by complexometric titration, X-ray diffraction (XRD), scamming electron microscopy (SEM) and transmission electron microscopy (TEM). It is demonstrated that the NiOOH with a flaky-like morphology are dispersed randomly on the surface of the spherical β-$Ni(OH)_2$. The effect of NiOOH on the electrochemical performance of spherical nonstoichiometric $Ni(OH)_x$ is studied by galvanostatic charge–discharge experiments and cyclic voltammetry. Compared with the spherical β-$Ni(OH)_2$, the spherical nonstoichiometric $Ni(OH)_x$ ($x = 2.05$) has an enhanced discharge capacity (300 mAh g^{-1} at 0.2 C), higher discharge potential plateau and superior cycle stability. The existence of chemically oxidized NiOOH nanoparticles in the nickel electrode contributes great effect on the improvement of electrochemical performance.

1. Introduction

Nickel–metal hydride (Ni/MH) batteries with high specific power and specific energy density are considered to be one of the most promising choices for electric vehicle (EV) and hydride electric vehicle (HEV) applications [1]. β-Nickel hydroxides are widely used as the positive material of Ni/MH batteries. However, β-$Ni(OH)_2$ is a kind of p-type semiconductor and its poor electronic conductivity handicaps the discharge ability of Ni/MH batteries [2]. Therefore, many attempts have been made to improve the electronic conductivity of $Ni(OH)_2$, such as the addition of zinc [3], cobalt [4–9], calcium [10], and yttrium elements [11–14] into the recipe of $Ni(OH)_2$ electrodes. Investigations have shown that the spherical β-$Ni(OH)_2$ particles coated with Co [4], $Co(OH)_2$ [5,6] and CoOOH [7] exhibit superior conductivity and better electrochemical performance. It is believed that Co or $Co(OH)_2$ is converted to a highly conductive CoOOH network on the surface of $Ni(OH)_2$ electrodes after chemical oxidation or electrochemical oxidation in the strong alkaline media [5,8,9].

It is well known that NiOOH is the oxidized or charged state of $Ni(OH)_2$. Among the four different phases over the lifetime of a nickel hydroxide electrode, β-$Ni(OH)_2$ is usually the starting active material which on charge transforms to β-NiOOH and on further charge or overcharge to γ-NiOOH. γ-NiOOH transforms to α-$Ni(OH)_2$ on discharge and vice versa on charge [15]. Recently, a new type of alkaline Zn/Ni batteries has been developed to meet the high power requirement for digital code portable electronics. Thus, the research of NiOOH as an individual electrode material for the alkaline Zn/Ni batteries has attracted a lot of interest. The NiOOH has good uniform morphology and high tap density, which can be obtained by chemical oxidation of spherical β-$Ni(OH)_2$ [16–19]. As the cathode electrode material of Zn/Ni batteries, NiOOH has excellent electrochemical activity during the charge-discharge cycling process [16–19]. Besides, nickel element has similar electrochemical property of cobalt. However, it has gained little attention for NiOOH as the additive material of nickel electrode in the past.

Based on the studies of NiOOH electrode of Zn/Ni batteries [16–19] and the proton exchange of layered $Ni(OH)_2$ [15,20,21], in our previous study, we prepared $Ni(OH)_x$ ($x = 2.01–2.15$) as new electrode materials for Ni/MH batteries through a simple route of chemical oxidation[22,23]. We found that the $Ni(OH)_x$ materials exhibit enhanced discharge capacity. It was indicated that chemically oxidized NiOOH can improve the electrochemical performance of nickel electrode. In addition, it has been documented that the overall activity of a battery depends on not only the microstructure but also the crystallite size and shape of the active material [24]. Nickel hydroxide with smaller crystalline size shows a high proton diffusion coefficient, giving excellent electrochemical performance [25]. It was reported that the specific capacity can be increased over 10% at 0.2 C when the active material was prepared

* Corresponding author. Tel.: +86 731 8887 9850; fax: +86 731 8887 9850.
E-mail address: huangkelong@163.com (K. Huang).

0378-7753/$ – see front matter © 2010 Elsevier B.V. All rights reserved.
doi:10.1016/j.jpowsour.2010.02.048

by mixing nano-scale $Ni(OH)_2$ with conventional spherical $Ni(OH)_2$ [25,26].

In this work, the spherical nonstoichiometric $Ni(OH)_x$ (x = 2.03–2.10) were synthesized by spherical β-$Ni(OH)_2$ surface modified with chemically oxidized NiOOH nanoparticles as the active materials of positive electrode for Ni/MH batteries. The electrochemical characterization of all the samples was carried out by galvanostatic charge–discharge experiments and cyclic voltammetry. It is anticipated that the chemically oxidized NiOOH nanoparticles can effectively enhanced the electrochemical performance of the spherical nonstoichiometric $Ni(OH)_x$.

2. Experimental

2.1. Synthesis of spherical nonstoichiometric $Ni(OH)_x$

The spherical β-$Ni(OH)_2$ used in this investigation was commercial obtainable β-$Ni(OH)_2$ product. In a typical synthesis test, the green $Ni(OH)_2$ powder was prepared as described previously [26]. Then the powder was added into a given amount of NaOH (2 M) and NaClO (10 wt%). After stirring for 2 h at room temperature, the precipitate was separated by centrifuge and rinsed with distilled water three times to remove the adsorbed ions. The washed precipitate was dried in a vacuum oven at 50 °C for 12 h. Finally, NiOOH of 97.2% purity was obtained as determined by the iodometry and EDTA titration. Then the spherical β-$Ni(OH)_2$ was coated with NiOOH by mechanical mixing for the nanoparticles could be well dispersed on the surface of spherical β-$Ni(OH)_2$. The amount of NiOOH coating ranged between 3 and 10 wt%, controlled by weight of NiOOH. The spherical β-$Ni(OH)_2$ was coated with the prepared $Ni(OH)_2$ by mechanical mixing for comparison.

The average nickel oxidation state was determined by iodometry and EDTA titration. Typically, 100 mg of the product was mixed with 2 g of KI and added into 0.5 M H_2SO_4 solution. The solution was then placed in the dark for 1 h, and the I_2 produced from the nickel reduction was titrated with 0.1 M $Na_2S_2O_3$ using starch as an indicator. 10% NH_3 solution was added to neutralize the excess acid, and NH_4Cl/NH_3 buffer solution was added (pH = 10) as well. The total amount of nickel was titrated with 0.1 M EDTA using murexide as an indicator. Each product was analyzed three times.

All the samples were characterized by X-ray diffraction (XRD, XD-98) using Cu Kα (1.5406 Å) radiation. The morphology was investigated with scanning electron microscope (SEM, JSM-6360LV) and transmission electron microscopy (TEM, JE01-1230).

2.2. Preparation of nickel electrodes and electrochemical measurements

The pasted $Ni(OH)_2$ electrodes were made by filling foam nickel substrates with a mixture of 80 wt% sample, 5 wt% CoO, 10 wt% Ni powder and 5 wt% PTFE. Solution of 6 mol L^{-1} KOH and 15 g L^{-1} LiOH was used as the electrolyte, a pure nickel wire as counter electrode and an Hg/HgO as reference electrode. Cyclic voltammetric studies were carried out in a three-electrode model cell at 25 °C using Princeton Applied Research 2273 electrochemical workstation. The charge–discharge test was carried out with a LAND CT2001A cell test instrument in a model test cell, including a pasted nickel electrode (1 cm × 1 cm) as the cathode, a standard AB_5-type hydrogen storage alloy electrode as the anode. For activation, the electrodes were charged at 0.2 C for 6 h and discharged at 0.2 C to a limited voltage of 0.9 V for 8 times. In the subsequent charge–discharge cycling tests, the electrodes were charged at 1 C for 1.2 h and discharged at 1, 2, 5 C. The corresponding cut-off voltages were set as 0.9 V.

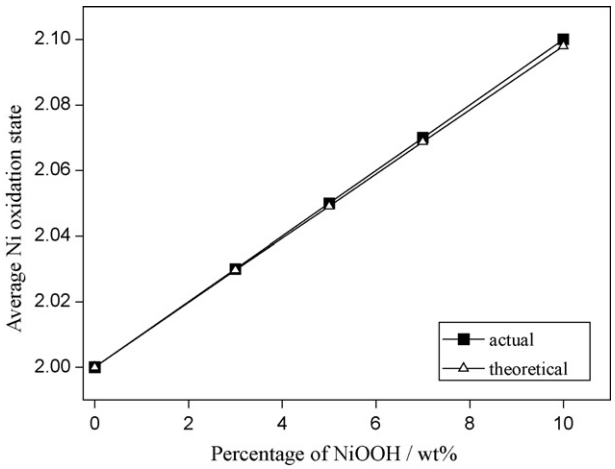

Fig. 1. Effect of the amount of NiOOH coating on the average Ni oxidation state.

3. Results and discussion

3.1. Characterization of the spherical nonstoichiometric $Ni(OH)_x$

Fig. 1 expresses the effect of the amount of NiOOH coating on the average Ni oxidation state (x) of the spherical nonstoichiometric $Ni(OH)_x$. It can be seen that x value increases with the increasing amount of NiOOH. Obviously, the x value is basically the same with the theoretical, which means that the Ni oxidation state has not been changed in the process of mechanical mixing. Furthermore, the spherical nonstoichiometric $Ni(OH)_x$ is a complex of Ni(II) and Ni(III) hydroxide.

Fig. 2 presents the XRD patterns of the spherical β-$Ni(OH)_2$ and nonstoichiometric $Ni(OH)_x$ (x = 2.03–2.10). No characteristic diffraction peak of γ-NiOOH is detected in the NiOOH sample, illustrating that NiOOH is a single phase of β-NiOOH. Clearly, the diffraction peak of the (0 0 2) plane of the β-NiOOH is identified when the x reaches 2.10. The diffraction peak of the (0 0 1) plane of the β-NiOOH should be observed at around 18.4°, although it appears to be hidden by the (0 0 1) plane of β-$Ni(OH)_2$. Moreover, the diffraction intensity of (0 0 1) planes of the β-$Ni(OH)_2$ decreases to a certain extent after coating with NiOOH. The difference in diffraction relative intensity between the samples indicates their difference in microstructure and morphology [27].

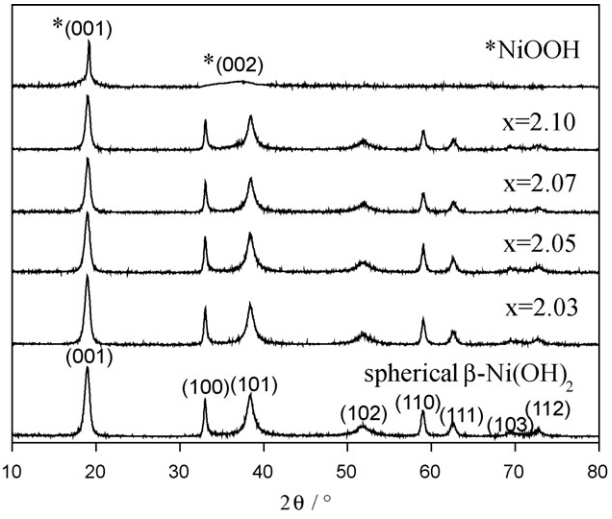

Fig. 2. XRD patterns of the spherical β-$Ni(OH)_2$, nonstoichiometric $Ni(OH)_x$ (x = 2.03–2.10) and prepared NiOOH.

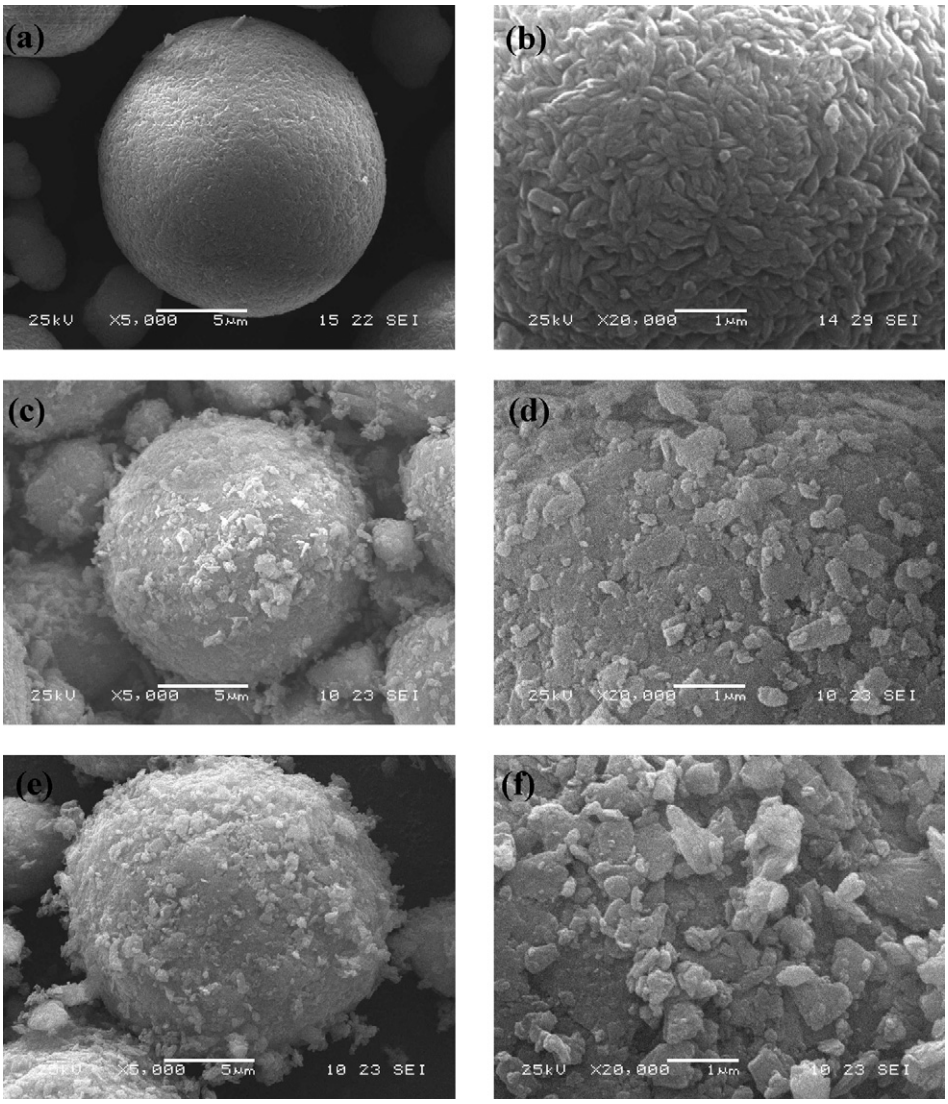

Fig. 3. SEM images of spherical β-Ni(OH)$_2$ (a and b), nonstoichiometric Ni(OH)$_x$: x = 2.05 (c and d) and x = 2.07 (e and f).

Representative SEM images of nonstoichiometric Ni(OH)$_x$ are given in Fig. 3. Compared with the spherical β-Ni(OH)$_2$, the surface of the nonstoichiometric Ni(OH)$_x$ (x = 2.05–2.07) in Fig. 3c–f become coarse with lots of flaky-like particles, though they still show sphere-like morphology. It is obviously that the irregular flaky-like particles are composed of NiOOH. Besides, with increasing of the coated amount of NiOOH, much more NiOOH particles are not coated in the surface of spherical β-Ni(OH)$_2$.

Typical TEM image of nonstoichiometric Ni(OH)$_x$ (x = 2.05) is illustrated in Fig. 4. The flaky-like NiOOH particles are dispersed randomly on the surface of the spherical β-Ni(OH)$_2$ microspheres. The thickness of the flake is in the range of 40–60 nm. The selected area electronic diffraction (SAED) in Fig. 4b exhibits diffraction patterns for the shell, which indicates that the shell is crystalline β-NiOOH. The nonstoichiometric Ni(OH)$_x$ are just Ni(OH)$_2$ covered with NiOOH shell. The structure of the material has not been changed in the process of mechanical mixing.

3.2. Electrochemical performance of the spherical nonstoichiometric Ni(OH)$_x$

Fig. 5 presents the relationship between the discharge capacity and the nonstoichiometric Ni(OH)$_x$ (x = 2.03–2.10) at different discharge rates after activation. Obviously, the discharge capacity at all the discharge rates (1, 2 and 5 C) of nonstoichiometric Ni(OH)$_x$ increases rapidly until the x value reaches 2.05, then reduces slightly. In the present study, the NiOOH nanoparticles seem to be a key factor for improving the discharge capacity of the nickel electrode. However, an excess amount of NiOOH leads to a decrease of the discharge capacity.

Fig. 6 shows the cycle performance of nonstoichiometric Ni(OH)$_x$ (x = 2.03–2.07). During these cycle processes, the nonstoichiometric Ni(OH)$_x$ (x = 2.03–2.07) show higher specific capacity and better cycling stability than the spherical β-Ni(OH)$_2$. The capacity fading of the nonstoichiometric Ni(OH)$_x$ (x = 2.03–2.07) are restricted to a very lower level after long-term cycling, while that of β-Ni(OH)$_2$ diminishes quickly. Especially, the discharge capacity of the nonstoichiometric Ni(OH)$_x$ (x = 2.05) is 289 mAh g^{-1}, much higher than the β-Ni(OH)$_2$ (186 mAh g^{-1}) at 2 C. After 200 cycles at 2 C, the discharge capacity of the nonstoichiometric Ni(OH)$_x$ (x = 2.05) remains as high as 279 mAh g^{-1}, but that of the spherical β-Ni(OH)$_2$ decreases a lot, only about 132 mAh g^{-1}. It indicates that the existence of chemically oxidized NiOOH enhances the cycling stability and extends the lifespan of the positive electrode at high-discharge rate. According to the cycle performance and discharge capacity, the optimal average Ni oxidation state in nonstoichiometric Ni(OH)$_x$ could be 2.05.

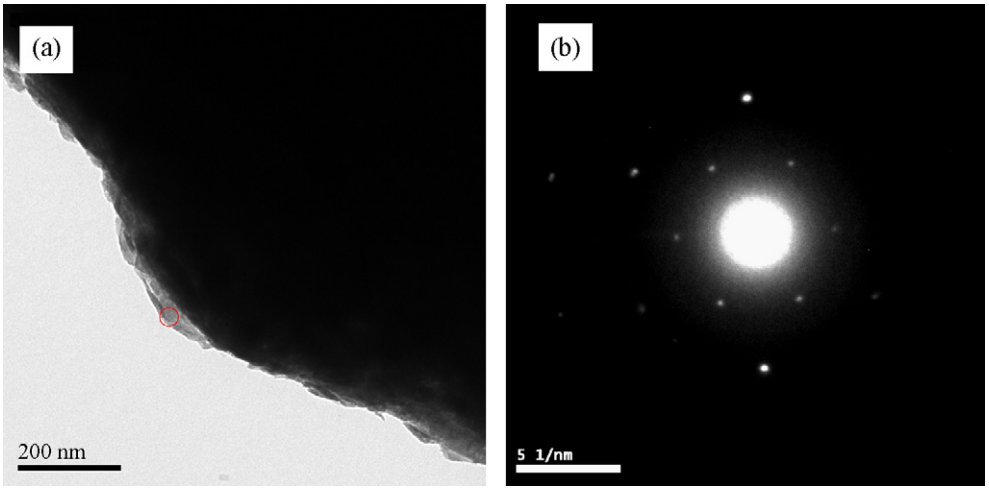

Fig. 4. TEM image (a) of nonstoichiometric $Ni(OH)_x$ ($x = 2.05$) and SAED pattern (b) of the particle boundary.

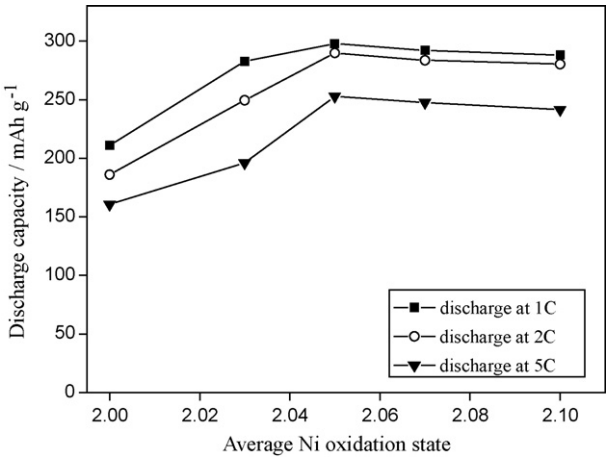

Fig. 5. The discharge capacity of spherical β-$Ni(OH)_2$ and nonstoichiometric $Ni(OH)_x$ ($x = 2.03$–2.10) at different discharge rates.

In order to further confirm the effect of NiOOH on the electrochemical performance of nonstoichiometric $Ni(OH)_x$, the electrochemical performance of the nonstoichiometric $Ni(OH)_x$ ($x = 2.05$) is further investigated in compare with the pure spherical β-$Ni(OH)_2$ and the spherical β-$Ni(OH)_2$ coated with 5 wt% prepared

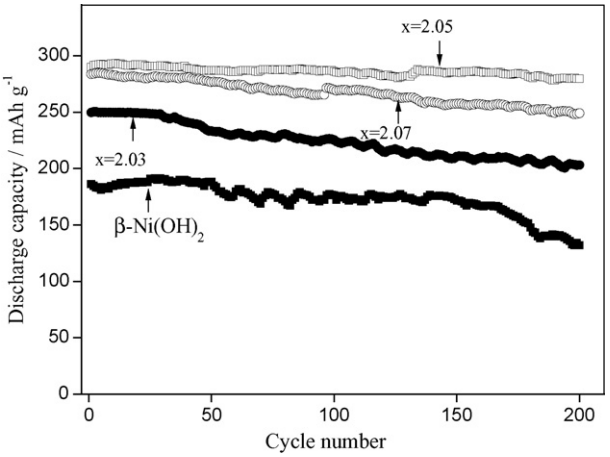

Fig. 6. Cycle performance of spherical β-$Ni(OH)_2$ and nonstoichiometric $Ni(OH)_x$ ($x = 2.03$–2.07) at 2 C.

$Ni(OH)_2$. Fig. 7 depicts the typical discharge curves of pure spherical β-$Ni(OH)_2$, spherical β-$Ni(OH)_2$ coated with 5 wt% prepared $Ni(OH)_2$ and nonstoichiometric $Ni(OH)_x$ ($x = 2.05$) at different discharge rates. Obviously, the nonstoichiometric $Ni(OH)_x$ ($x = 2.05$) exhibits a larger discharge capacity and higher discharge potential plateau than the others at the same discharge rate (0.2, 1, 2 and 5 C). The discharge capacity of nonstoichiometric $Ni(OH)_x$ ($x = 2.05$) increases from 242 to 300 mAh g^{-1} at 0.2 C, while the coated with 5 wt% prepared $Ni(OH)_2$ sample is only 268 mAh g^{-1}. It illustrates that in addition to the phase transformation of β-$Ni(OH)_2$ to β-NiOOH, partial formation of γ-NiOOH was occurred [28,29] in the charge–discharge process of nonstoichiometric $Ni(OH)_x$ ($x = 2.05$). Moreover, the discharge capacity of the nonstoichiometric sample is about 253 mAh g^{-1} at 5 C, much higher than that of the spherical β-$Ni(OH)_2$ (161 mAh g^{-1}) and the coated with 5 wt % prepared $Ni(OH)_2$ sample (184 mAh g^{-1}), which is beneficial to the high power of Ni/MH batteries. The improvement of the discharge capacity, high-rate discharge ability, and high discharge potential plateau is due to the coating NiOOH.

The cyclic voltammograms of the three samples after full activation with the scan rate of 0.2 mV s^{-1} are illustrated in Fig. 8. The features of the voltammograms are summarized in Table 1. Obviously, the oxidation potential peak of the nonstoichiometric $Ni(OH)_x$ ($x = 2.05$) shifts to a more negative position at 522 mV and the reduction potential peak moves to a more opposite site at 302 mV in compare with that of the spherical β-$Ni(OH)_2$, corresponding to the above discharge curves with a higher discharge potential plateau. The potential difference between the oxidation and reduction peaks (E_O–E_R) for the nonstoichiometric $Ni(OH)_x$ ($x = 2.05$) is much smaller than that of spherical β-$Ni(OH)_2$ and the coated with 5 wt% prepared $Ni(OH)_2$ one, indicating better reversibility of the electrochemical redox reaction in the nonstoichiometric sample. Meanwhile, the potential difference between the oxygen evolution potential and the oxidation potential (E_{OE}–E_O)

Table 1
Electrochemical parameters from CVs of the samples.

Electrode	Potential (mV)				
	E_R	E_O	E_{OE}	E_O–E_R	E_{OE}–E_O
Spherical β-$Ni(OH)_2$	282	551	621	269	70
Nonstoichiometric $Ni(OH)_x$ ($x = 2.05$)	302	522	615	220	93
β-$Ni(OH)_2$ coated with 5 wt% prepared $Ni(OH)_2$	289	532	619	243	87

E_R: reduction potential; E_O: oxidation potential; E_{OE}: oxygen-evolution potential.

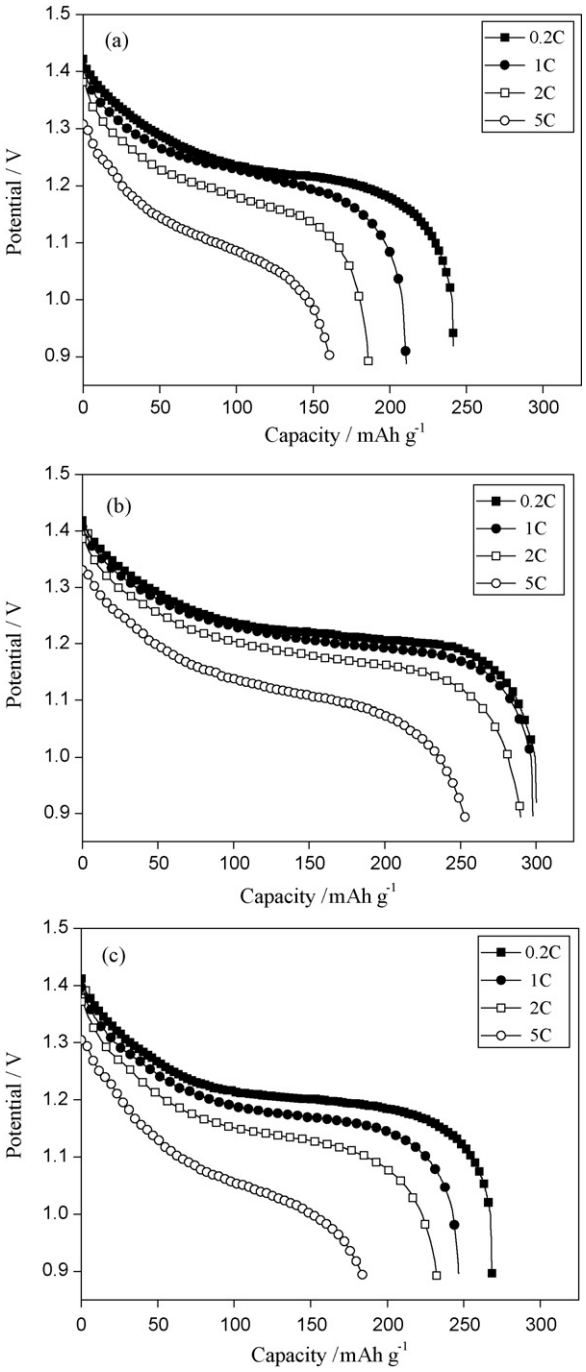

Fig. 7. Discharge curves of spherical β-$Ni(OH)_2$ (a), nonstoichiometric $Ni(OH)_x$ (x = 2.05) (b) and spherical β-$Ni(OH)_2$ coated with 5 wt% prepared $Ni(OH)_2$ (c) at different discharge rates.

becomes larger for the nonstoichiometric sample. This allows the nonstoichiometric one to be charged fully before oxygen evolution, which improves the charge efficiency [30]. Consequently, the overall electrochemical performance of the nonstoichiometric $Ni(OH)_x$ (x = 2.05) is obviously superior to the spherical β-$Ni(OH)_2$ and the coated with 5 wt% prepared $Ni(OH)_2$ sample.

The interesting question is why the nonstoichiometric $Ni(OH)_x$ show better comprehensive performance. An interpretation follows. In the first charge–discharge cycle, the chemically oxidized NiOOH nanoparticles with a high degree of disorder on the surface possess superior surface activities, which have enhanced electronic conductivity. In addition, the mixed-valence nickel exhibits

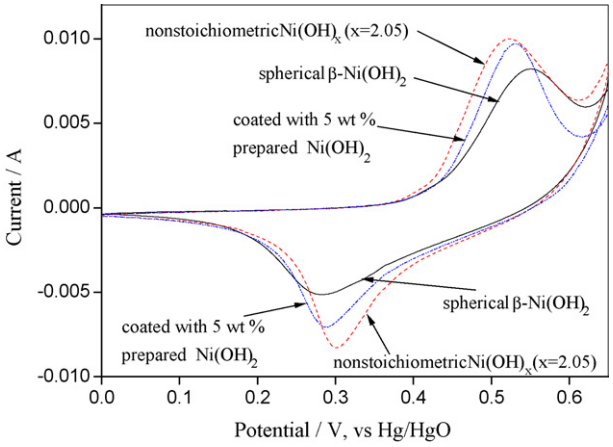

Fig. 8. CV curves of spherical β-$Ni(OH)_2$, nonstoichiometric $Ni(OH)_x$ (x = 2.05) and spherical β-$Ni(OH)_2$ coated with 5 wt% prepared $Ni(OH)_2$ with the scan rate of 0.2 mV s^{-1}.

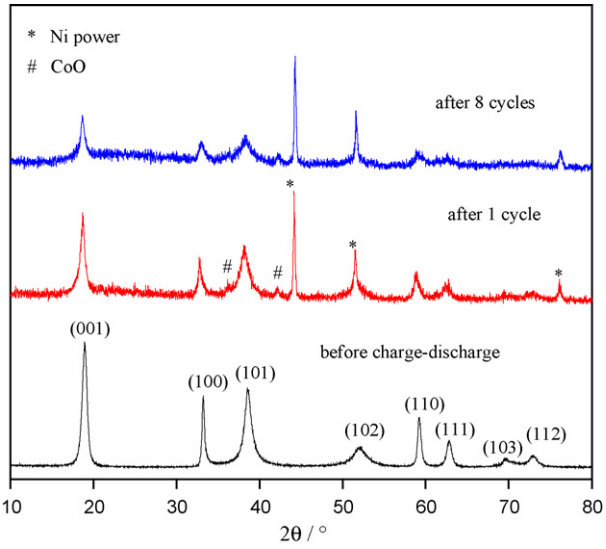

Fig. 9. XRD patterns of the nonstoichiometric $Ni(OH)_x$ (x = 2.05) after different cycles at 0.2 C.

higher activities for oxygen diffusion, which facilitates the oxidation of nickel(II) species into nickel(III or IV) and increases the discharge capacity of the nonstoichiometric $Ni(OH)_x$, similar to that of $Ni(OH)_2$ electrodes coated with CoOOH [31,32].

Fig. 9 presents the XRD patterns of the nonstoichiometric $Ni(OH)_x$ (x = 2.05) carried out after different cycles at 0.2 C in the present study. As Fig. 9 shows, the peaks corresponding to all the reflections in the XRD pattern of nonstoichiometric $Ni(OH)_x$ (x = 2.05) after charge–discharge are slightly broadened compared to those before charge–discharge, indicating the poor crystallinity after charge–discharge and good electrochemical activity [33]. The abnormal width of (0 0 1) and (1 0 1) reflections are caused by the existence of defects in the material [34]. It illustrates that the structure of the material has been changed in the process of change-discharge cycles with chemically oxidized NiOOH.

Fig. 10a shows the TEM image of nonstoichiometric $Ni(OH)_x$ (x = 2.05) after 8 cycles at 0.2 C. After charge–discharge cycles, the active material still shows sphere-like morphology coated with some flaky-like nanoparticles. Meanwhile, the flaky-like nanoparticle has a small crystal size and large surface area, which helps to enhance the contact between the active material and the electrolyte and allows proton diffusion to occur easily. Fig. 10b and c exhibit

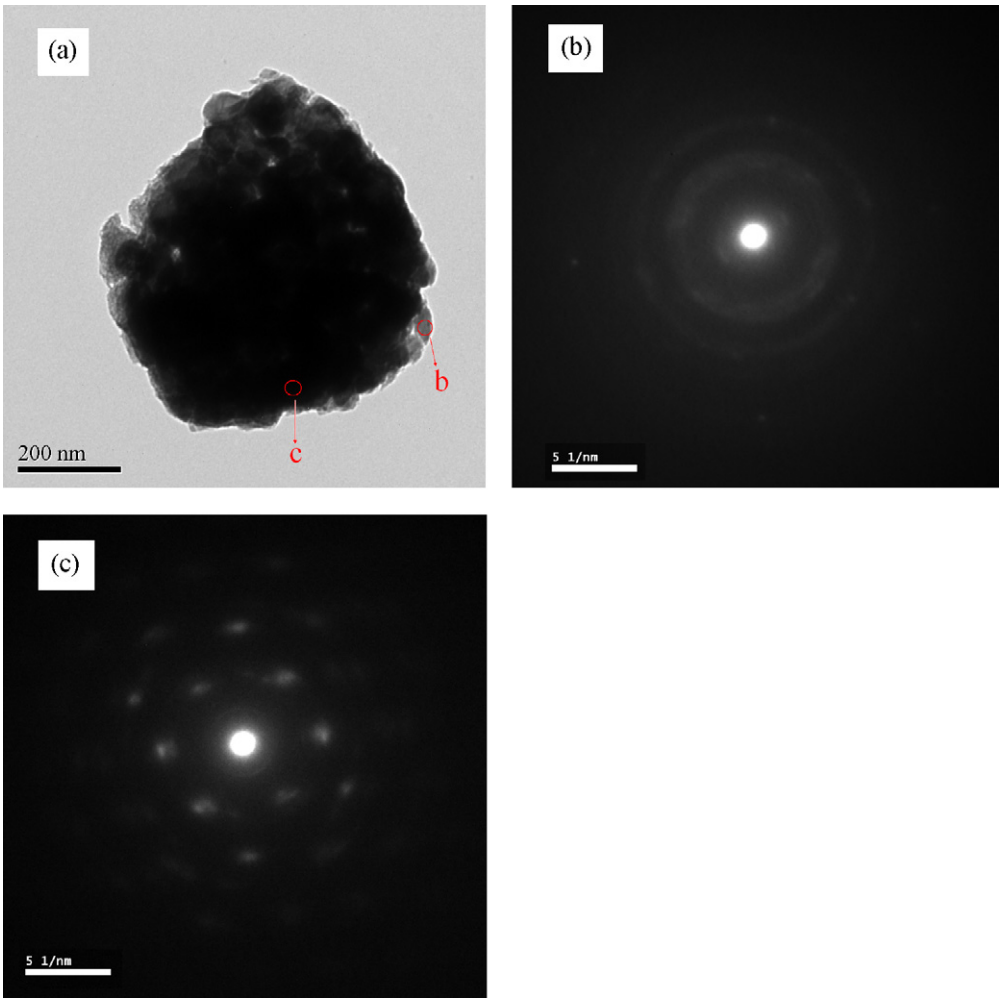

Fig. 10. TEM image (a), SAED patterns of the particle boundary (b) and bulk region (c) of nonstoichiometric $Ni(OH)_x$ ($x = 2.05$) after 8 cycles at 0.2 C.

diffraction patterns for the shell and particle of the nonstoichiometric $Ni(OH)_x$ ($x = 2.05$) after 8 cycles at 0.2 C, which indicate that the shell is badly crystalline $Ni(OH)_2$ and the particle is poor crystalline β-$Ni(OH)_2$. It illustrates that the chemically oxidized NiOOH transfers into badly crystalline $Ni(OH)_2$ and the structure of the material has been changed in the process of charge–discharge cycles, in agreement with the XRD analyses. Furthermore, the chemically oxidized NiOOH may cause changes in the electronic properties in charge–discharge cycles and the flaky-like nanoparticles act as a barrier for electron transfer in the oxygen-evolution process, which contributes to superior electrode performance at high current density.

On the basis of these facts, it can be concluded that chemically oxidized NiOOH nanoparticles coating is a key factor for improving the electrochemical performance of the spherical nonstoichiometric $Ni(OH)_x$ material, such as the discharge capacity, high-rate discharge ability, and cycle stability. On the other hand, the coated amount of NiOOH particles needs to be optimized to achieve the high discharge capacity of the coated electrode. Work in progress is to obtain a detailed understanding of the mechanism of chemically oxidized NiOOH on the nickel electrode.

4. Conclusion

The spherical nonstoichiometric $Ni(OH)_x$ ($x = 2.03$–2.10) were synthesized by mechanical mixing. Complexometric titration, XRD, SEM and TEM observations show that the flaky-like NiOOH nanoparticles are dispersed randomly on the surface of the spherical β-$Ni(OH)_2$. The electrochemical measurements demonstrate that the coating layer of NiOOH can effectively improve the electrochemical performance of spherical nonstoichiometric $Ni(OH)_x$. The spherical nonstoichiometric $Ni(OH)_x$ ($x = 2.05$) has the highest discharge capacity, enhanced high-rate discharge ability and improved cycle stability. The discharge capacity of the sample can reach 300 mAh g^{-1} at 0.2 C and about 253 mAh g^{-1} at 5 C. Besides, more than 96% of its initial capacity is retained after 200 cycles at 2 C. The CV tests reveal that the spherical nonstoichiometric $Ni(OH)_x$ ($x = 2.05$) also has a high electrochemical reaction activity and good reversibility, and these properties contribute to the excellent electrochemical performance. The results suggest that the spherical nonstoichiometric $Ni(OH)_x$ can be considered as a new positive electrode material for Ni/MH batteries.

Acknowledgement

The work was financially supported by the National Natural Science Foundation of China (No. 50772133).

References

[1] U. Köhler, J. Kümpers, M. Ullrich, J. Power Sources 105 (2002) 139–144.
[2] D.M. Constantin, E.M. Rus, L. Oniciu, L. Ghergari, J. Power Sources 74 (1998) 188–197.
[3] C. Tessier, C. Faure, L.G. Demourgues, C. Denage, G. Nabias, C. Delmas, J. Electrochem. Soc. 149 (2002) A1136–A1145.

[4] A.B. Yuan, S.A. Cheng, J.Q. Zhang, C.N. Cao, J. Power Sources 77 (1999) 178–182.
[5] M. Oshitani, H. Yufu, K. Takashima, S. Tsuji, Y. Matsumaru, J. Electrochem. Soc. 136 (1989) 1590–1593.
[6] Z.R. Chang, H.W. Tang, J.G. Chen, Electrochem. Commun. 1 (1999) 513–516.
[7] W.K. Hu, X.P. Gao, M.M. Geng, Z.X. Gong, D. Noréus, J. Phys. Chem. B 109 (2005) 5392–5394.
[8] V. Pralong, A. Delahaye-Vidal, B. Beaudoin, B. Gerand, J.M. Tarascon, J. Mater. Chem. 9 (1999) 955–960.
[9] F. Bardé, M.R. Palacin, B. Beaudoin, A. Delahaye-Vidal, J.M. Tarascon, Chem. Mater. 14 (2004) 299–306.
[10] X.M. He, J.G. Ren, W. Li, C.Y. Jiang, C.R. Wan, Electrochim. Acta 51 (2006) 4533–4536.
[11] F.Y. Cheng, J. Chen, P.W. Shen, J. Power Sources 150 (2005) 255–260.
[12] K. Shinyama, H. Nakamura, T. Nohma, I. Yonezu, J. Alloys Compd. 408 (2006) 288–293.
[13] J. Fan, Y.F. Yang, Y.B. Yang, H.X. Shao, Electrochim. Acta 53 (2007) 1979–1986.
[14] J. Fan, Y.F. Yang, P. Yu, W.H. Chen, H.X. Shao, J. Power Sources 171 (2007) 981–989.
[15] H. Bode, J. Dehmelt, Electrochim. Acta 11 (1966) 1079–1087.
[16] J.Q. Pan, Y.Z. Sun, P.Y. Wan, Z.H. Wang, X.G. Liu, Electrochem. Commun. 7 (2005) 857–862.
[17] F. Bardé, M.R. Palacín, B. Beaudoin, P.A. Christian, J.M. Tarascon, J. Power Sources 160 (2006) 733–743.
[18] E. Skipworth, S.W. Donne, J. Power Sources 174 (2007) 186–190.
[19] L.P. Liu, Z.T. Zhou, C.H. Peng, Electrochim. Acta 54 (2008) 434–441.
[20] A. Van der Ven, D. Morgan, Y.S. Meng, G. Ceder, J. Electrochem. Soc. 153 (2006) A210–A215.
[21] B. Mavis, M. Akinc, Chem. Mater. 18 (2006) 5317–5325.
[22] X.L. Zhong, K.L. Huang, S.Q. Liu, Y.J. Li, D.Y. Chen, Chin. J. Inorg. Chem. 25 (2009) 19–25.
[23] X.L. Zhong, H.N. Qin, K.L. Huang, S.Q. Liu, Acta Chim. Sin. 12 (2009) 1343–1348.
[24] M. Figlarz, B. Gérand, A. Delahaye-Vidal, B. Dumont, F. Harb, A. Coucou, F. Fievet, Solid State Ionics 43 (1990) 143–170.
[25] X.H. Liu, L. Yu, J. Power Sources 128 (2004) 326–330.
[26] X.Y. Guan, J.C. Deng, Mater. Lett. 61 (2007) 621–625.
[27] D.L. Chen, L. Gao, Chem. Phys. Lett. 405 (2005) 159–164.
[28] N. Sac-Epée, M.R. Palacin, A. Delahaye-Vidal, Y. Chabre, J.-M. arascon, J. Electrochem. Soc. 145 (1998) 1434–1441.
[29] F. Bardé, M.R. Palacin, Y. Chabre, O. Isnard, J.M. Tarascon, Chem. Mater. 16 (2004) 3936–3948.
[30] W.H. Zhu, J.J. Ke, H.M. Yu, D.J. Zhang, J. Power Sources 56 (1995) 75–79.
[31] V. Pralong, A. Delahaye-Vidal, B. Beaudoin, J.B. Leriche, J.M. Tarascon, J. Electrochem. Soc. 147 (2000) 1306–1313.
[32] W.K. Hu, X.P. Gao, D. Noréus, T. Burchardt, N.K. Nakstad, J. Power Sources 160 (2006) 704–710.
[33] R.S. Jayashree, P.V. Kamath, G.N. Subbanna, J. Electrochem. Soc. 147 (2000) 2029–2032.
[34] C. Delmas, C. Tessier, J. Mater. Chem. 7 (1997) 1439–1443.